Journal of Hazardous Materials Advances 23 (2026) 101469

Contents lists available at ScienceDirect

Journal of Hazardous Materials Advances

journal homepage: www.elsevier.com/locate/hazadv

Pre-industrial mercury exposure in early modern Europe: integrating hair Hg, stable isotopes, and burial geochemistry from a 17th-century plague mass grave

Fabrizio Monaci [a,b,*], Riccardo Fedeli [a], Kaylie Anne Walsh [a], Melanie Langbein [c], Julian Decker [d]

[a] Department of Life Science, University of Siena, Via P.A. Mattioli 4, Siena, 53100, Italy
[b] National Biodiversity Future Center (NBFC), 90133, Palermo, Italy
[c] Stadt Nürnberg, Bauordnungsbehörde, Stadtarchäologie, Bauhof 5, 90402, Nürnberg, Germany
[d] In Terra Veritas GmbH, Ottostraße 15, 96047 Bamberg, Germany

ARTICLE INFO

Keywords:
Mercury
Mercury exposure
Stable isotopes
Scalp-hair
Paleotoxicology
Taphonomy
Bioarcheology

ABSTRACT

Human mercury (Hg) exposure in pre-industrial Europe remains poorly quantified, despite widespread therapeutic and artisanal use during the early modern period (ca. 1500–1800). We combined hair total Hg (THg), bulk stable isotopes ($\delta^{13}C$, $\delta^{15}N$, $\delta^{18}O$), and burial-sediment geochemistry to reconstruct Hg exposure in a 17th-century mass grave in Nuremberg, Germany (1632–1634). X-ray fluorescence identified three sediment facies, including a metal-enriched backfill; elemental Hg^0 droplets, probably from medical pills, were observed in the fill, raising post-burial contamination concerns. Hair from a low-Hg facies distinct from these deposits, was decontaminated (validated by a paired washed/dry-brushed comparison); reported THg values are upper bounds on ante-mortem exposure. Hair THg ranged 0.51–3.38 μg g^{-1} (median 1.63; n = 15), 80% exceeding 1.0 μg g^{-1}. $\delta^{13}C$ and $\delta^{15}N$ values are consistent with homogeneous terrestrial C3-based diets. Systematic ^{15}N enrichment may partly reflect ante-mortem catabolism associated with famine and illness, although a contribution from animal-protein intake cannot be excluded. In a multivariable model, THg covaried weakly with $\delta^{13}C$ but not with $\delta^{15}N$ or $\delta^{18}O$; this exploratory trend, sensitive to a single influential individual, is compatible with mixed exposure routes and a limited dietary contribution. Narrow clustering of $\delta^{18}O$ shows no clear geographic heterogeneity, consistent with Hg burden being driven primarily by local factors (e.g. therapeutic or occupational exposure) rather than by access to isotopically distinct water sources. These rare pre-industrial hair-Hg benchmarks suggest exposure higher than in most modern populations. Given the small sample size (n = 15) and possible selection effects, these findings should be interpreted as exploratory.

1. Introduction

Mercury (Hg) is a persistent, bioaccumulative contaminant whose environmental burden has been substantially increased throughout the globe by human activities. Since the Industrial Era (ca. 1850), anthropogenic emissions have raised the total atmospheric Hg burden roughly threefold and increased deposition to terrestrial and aquatic ecosystems by about fourfold (Driscoll et al., 2013; Gustin et al., 2020; Streets et al., 2017). In fact, Hg contamination predated the Industrial Revolution, with localized enrichment occurring centuries before industrialization or even millennia earlier in areas with cinnabar (HgS) and precious-metal mining (Cooke et al., 2020; Corella et al., 2021), such as Almadén in Spain, where measurable atmospheric enrichment have started as early as 2500 years ago and intensified during Roman and Medieval periods (Martínez-Cortizas et al., 1999).

Human exposure to Hg in early modern Europe (ca. 1500–1800) likely differed substantially from present-day exposure patterns. In that period, the principal hazard was inhalation of elemental Hg vapour, affecting miners and craft workers who handled Hg in trades such as hat-felting and mirror silvering (García Gómez et al., 2007; Kobal et al., 2017; Lombardi et al., 2012; WHO, 1991). A second major route of exposure was the therapeutic administration of inorganic Hg

* Corresponding author at: Department of Life Science, University of Siena, Via P.A. Mattioli 4, Siena, 53100, Italy.
E-mail address: fabrizio.monaci@unisi.it (F. Monaci).

https://doi.org/10.1016/j.hazadv.2026.101469
Received 8 February 2026; Received in revised form 2 August 2026; Accepted 4 August 2026
Available online 5 August 2026

compounds that physicians prescribed for the treatment of syphilis or various dermatological conditions (pediculosis, scabies; Apelbaum, 2021; Fornaciari et al., 2011) while dietary exposure occurred especially in communities inhabiting mining areas, where contamination of freshwater fish was responsible for high methylmercury (MeHg) loads (Wiener and Suchanek, 2008). Such a historical exposure profile appears to differ remarkably from the contemporary one, where fish consumption is the main cause of Hg body burden increase in non-occupationally exposed populations (Esteban et al., 2015; Wu et al., 2024). However, the relative contribution of dietary, occupational, and therapeutic pathways of human exposure to Hg in early modern times remain poorly understood and likely was varying with location, socioeconomic conditions, occupation and individual medical history (Lombardi et al., 2012; Zillioux, 2015).

Hair total mercury (THg) is the primary biomarker for recent MeHg exposure, and a standardized European analytical framework improves comparability across studies (Esteban et al., 2015). Because MeHg is efficiently absorbed and incorporated during keratinization, it typically constitutes 80–95% of hair THg in fish-consuming populations, whereas inorganic Hg contributes little (WHO, 1991, 1990). Hair Hg isotopes can further distinguish dietary MeHg from inhaled elemental Hg, enabling source apportionment (Du et al., 2021; Wang et al., 2023).

Because hair keratin records exposure during the weeks to months preceding death, a finer temporal resolution than the multi-year average bone collagen, scalp hair is the material of choice for archaeological studies of diet, mobility, and individual life histories (Bleasdale et al., 2019; Lorentz et al., 2020; Macko et al., 1999; Wang et al., 2022; Wilson et al., 2007). Its stable carbon, nitrogen, and oxygen isotope analysis correspondingly reveal diet, metabolic status, and movements within this window: in temperate European contexts bulk hair isotopes reflect terrestrial C3 diets with variable animal-protein and freshwater-fish input (Hakenbeck et al., 2010; Morrone et al., 2023); δ^{15}N can mark catabolic protein recycling during prolonged illness and famine, particularly when accompanied by stable or slightly decreased δ^{13}C indicating lipid mobilization (Eerkens et al., 2017; Neuberger et al., 2013; Walter et al., 2020); and δ^{18}O tracks body water, and hence drinking-water sources and mobility (Bowen, 2010; Ehleringer et al., 2008; Kennedy et al., 2011; O'Brien and Wooller, 2007). Keratin diagenesis can nonetheless compromise δ^{18}O values under wet burial conditions, so cautious interpretation is essential (Auerswald et al., 2011; Capuzzo et al., 2025; Von Holstein et al., 2014).

In contrast, most of archaeological Hg research has relied on bone, which is not a primary target for Hg accumulation, and whose Hg content reflects not only lifetime exposure but also turnover, mineral-organic composition, and post-burial alteration (Álvarez-Fernández et al., 2022). Keratinized tissues, by contrast, record systemic Hg burdens near death without remodelling, but archaeological hair studies remain scarce because of limited preservation and taphonomic complexity: post-depositional surface enrichment can occur (Zvereva et al., 2017), and decomposing skeletal tissues can act as transient Hg reservoirs influencing adjacent keratin (Alvarez-Fernandez et al., 2022). Rigorous decontamination is therefore essential.

When taphonomic factors that may affect hair signals are taken into account, THg hair-based reconstructions can clarify historical exposure pathways (Du et al., 2021; Wang et al., 2022; Zvereva et al., 2017) or capture short-term nutritional stress through stable isotope analysis (Neuberger et al., 2013; Walter et al., 2020). Integrating the two analytical approach would be particularly valuable especially in epidemic contexts such as medieval plague outbreaks, where nutritional stress has been singled out as a critical modifier of disease susceptibility and survival (DeWitte et al., 2025). No prior work, as far as we are aware, has paired THg concentrations with bulk C, N and O stable isotopes (e.g. δ^{13}C-δ^{15}N-δ^{18}O) to reconstruct exposure pathways together with dietary and physiological context. This knowledge gap has so far limited the interpretation of Hg exposure during epidemic crises and its relationships with nutritional status, mobility, and mortality. Moreover, the scarcity of archaeological hair-Hg dataset precludes the definition of a reference interval of pre-industrial hair-Hg concentration necessary to contextualize modern biomonitoring and Anthropocene Hg cycling.

To address these limitations, we conducted a biogeochemical investigation of hair samples from the 17th-century plague mass grave in Nuremberg, Germany. This burial assemblage, precisely dated to 1632–1634, included ca. 3000 individuals with an exceptional degree of preservation that have provided unprecedented quantities of keratinous tissue, useful to capture the temporal snapshot of the mortality event. Nevertheless, the grave also posed a major taphonomic challenge as it was partially filled with metalliferous artisanal/industrial waste with occasional elemental Hg (Hg^0) droplets that could have originated from mineralogical mobilization or through contamination via burst Hg filled pills used as medication at the time and carried in pouches that the deceased were buried with. Our main objectives were: (*i*) characterizing the burial-sediment layers to inform about the potential bias of hair THg concentrations via post-burial sorption; (*ii*) quantifying THg in decontaminated hair and validating decontamination effectiveness through a paired washed/dry-brushed comparison, to constrain the exogenous Hg contribution; and (*iii*) testing inter-individual THg variability in relation to dietary proxies such as δ^{13}C-δ^{15}N-δ^{18}O to assess whether it was associated with diet and mobility indicators, as it is expected under the MeHg-dominated exposure hypothesis, or decoupled from them, which would be consistent with the mixed non-dietary exposure routes hypothesis. Given the constraints of archaeological hair material and the resulting sample size, this study is framed as an exploratory, hypothesis-generating assessment rather than a population-representative survey.

2. Materials and methods

2.1. The Nuremberg plague mass grave (1632–1634)

Construction work in Nuremberg's St. Johannis District (2023–2024) uncovered a complex of eight mass graves containing ca. 3000 people who died during the 1632–1634 plague outbreak (Fig. 1). The epidemic killed >15,000 people, one-third of Nuremberg's population, making it Central Europe's most severe documented demographic crisis. Numismatic evidence from coins recovered from the pits, written sources and radiocarbon dating allowed a precise chronological assignment of the mortality event to the plague wave that spread across central and western Europe throughout the Thirty Years' War, causing a widespread increase in urban mortality due to the combination of epidemic disease and the aftermath of war (Alfani and Murphy, 2017). Rapid burials in emergency conditions, primarily using sandy soil, contributed to an exceptional preservation of organic materials (e.g., textile materials and keratinous tissues) and resulting in an outstanding opportunity for investigating human exposure to Hg within a defined epidemic mortality assemblage.

The excavation was carried out ahead of construction work, under the Bavarian Monument Protection Act (BayDSchG) by the competent municipal authority (Stadtarchäologie, Building Regulations Authority of the City of Nuremberg; co-author M. Langbein, City Archaeologist) and is registered under the Bavarian archaeological project reference M-2023–1729–1; as the study involved archaeological human remains and no living subjects, no ethics-board approval was required, and sampling, storage and curation followed recognised bioarcheological best practices (Squires et al., 2019).

2.2. Hair sampling and preparation

2.2.1. Sample collection

Hair specimens were collected during controlled excavation (December 2024) using solvent-cleaned scalpels and forceps under powder-free nitrile glove protocols. Scalp portions with intact strands were selected; samples with excessive adherent material, visible damage, mineral encrustation, or severe keratin degradation were excluded.

Fig. 1. Study site position and archaeological setting. Excavation of 17th-century plague mass grave, Nuremberg, Germany (1632 - 1634), showing skeletal remains and site location (Photos: In Terra Veritas GmbH - Google Earth).

Although the assemblage comprises ca. 3000 individuals, intact scalp hair was preserved in only a small minority of burials, and well-preserved strands suitable for combined THg and triple-isotope ($\delta^{13}C$, $\delta^{15}N$, $\delta^{18}O$) measurement were available for far fewer. After applying the exclusion criteria above, 15 individuals retained sufficient analytically suitable material. The sample is therefore constrained by preservation rather than by analytical cost and is treated here as an exploratory series rather than a population-representative one. Contextual data included grave identification, stratigraphic layer, depth, anatomical associations, and osteological age/sex determinations where possible.

Preserved hair segments were approximately 4 cm long (range: 3–6 cm), corresponding to roughly 3–6 months prior to the time of death, given mean scalp hair elongation rates of 0.8–1.5 cm per month (Pragst and Balikova, 2006). Since hair orientation could not be ascertained, fragments from each individual were processed and analysed together with this peri-mortem interval, similar to archaeological samples in which preservation precludes fine-scale sampling (Bleasdale et al., 2019). In those cases where sufficient material was available, two aliquots were created per individual: one washed for chemical and isotopic analyses and one unwashed voucher as reference for future use. All aliquots were transferred to acid-cleaned glass in accordance with established procedures for human-hair isotope analyses (Coplen and Qi, 2012).

Sediment samples were obtained from three spatially distinct areas representing the heterogeneous burial matrix: (*i*) general fill material at the periphery of gravesides ("general fill"; Sed1); (*ii*) sediment directly associated with skeletal preservation including intact hair ("near-corpse"; Sed2); and (*iii*) locations exhibiting visible Hg^0 droplets ("Hg^0-bearing"; Sed3). Bulk (composite) samples were taken with solvent-cleaned stainless-steel hand tools by pooling five subsamples collected within approximately 1 m^2 and then placed into acid-washed borosilicate glass containers with PTFE lined caps and stored at 4 °C until analysis.

2.2.2. *Hair decontamination protocol*

Hair segments were processed using a Triton X-100-ethanol method commonly used for human-hair isotope reference materials (Coplen and Qi, 2012), which was compatible with Hg quantification (Aranda, 2008; Martinis and Wuilloud, 2010); modern preference for no-wash protocols in biomonitoring had been set aside due to the metalliferous burial environment which necessitated detergent-solvent decontamination to separate biogenic from diagenetic metal signals. Hg assessments were based on a QA/QC system in compliance with general European hair-Hg biomonitoring guidelines (Esteban et al., 2015), which involved the consideration of routine batch controls and pre-established acceptance criteria.

Following manual removal of visible matter with stainless steel instruments, specimens were soaked in 0.5% (*v/v*) Triton X-100 (ultrapure water, 18.2 MΩ·cm) and gently stirred for 30 min at room temperature. Samples were subsequently washed with 10 mL ultrapure water (5 times per samples, inverting them 30 times) and then placed in high-quality ethanol (≥99.9%) shaking them at low rotational speed for 12 h. The material was homogenized by cryogenic milling at -80 °C (Retsch MM 400 mill) after drying in a vented oven at 35 °C, a more conservative temperature than commonly used protocols (Yamakawa et al., 2025) to minimise any potential Hg loss during pre-treatment.

2.3. *Elemental characterization of burial sediments*

Elemental analysis of sediments was performed using X-ray fluorescence spectrometry (Olympus Vanta) with an X-ray tube of 4 W Rh anode at the excitation voltage from 10 to 50 kV. Sediments were air dried, homogenised by agate grinding, and sieved at 2-mm through stainless steel mesh, to have a homogeneous material. The sediment preparation of ca. 5 g was packed in XRF sample cups, sealed with 4 µm polypropylene foil windows. Analyses were performed using *Geochem* mode with 60 s acquisition per beam to ensure good sensitivity over the entire elemental range (Mg to U).

Four procedure assured data quality: energy calibration against the manufacturer's 316 stainless-steel reference disc; analysis of a certified reference material (Fedeli et al., 2024); replicate measurement of every sample; and periodic verification of Si detector stability. Repeatability, expressed as relative standard deviation, remained below 10% for major elements and below 15% for trace elements.

2.4. Total Hg analysis of hair

THg was quantified with a direct mercury analyser (DMA-80, Milestone s.r.l., Italy) which couples thermal decomposition, gold-trap amalgamation and thermal desorption to atomic absorption detection at 253.7 nm. Dried hair segments (3–10 mg) were weighed into pre-combusted quartz boat.

The following quality control materials were included in every analytical run: (*i*) instrument blanks, (*ii*) certified reference materials (NIST 2976, Mussel Tissue), (*iii*) in-house pooled hair controls, and (*iv*) sample duplicates. Multi-point aqueous calibration used NIST-traceable standards and documented CRM validation every seven determinations. Acceptable quality criteria were CRM recoveries between 90 and 110%, and duplicate percent relative standard deviation (RSD) values <10%. Blank-corrected mercury readings were batch-level with duplicate means when blanks met acceptance criterions.

2.4.1. Validation of the decontamination approach

To quantify the exogenous contribution to measured THg, archived unwashed voucher aliquots (Section 2.2.1) were used in a paired comparison. For seven individuals with sufficient material, one aliquot underwent dry mechanical removal of adherent matter only (dry-brushing), while the paired aliquot received the full detergent-solvent treatment described in Section 2.2.2. THg was determined on both aliquots on the same DMA-80 instrument and under identical calibration to preserve comparability. The difference between dry-brushed and fully washed aliquots estimates the removable, surface-associated Hg fraction, whereas the washed concentration represents the Hg retained after decontamination, on which all reported values are based. Because unwashed aliquots could reach high Hg concentrations, sample mass was reduced for the most concentrated specimens (below 1 mg for the highest-Hg sample) to keep Hg loading within the DMA-80 working range; instrument blanks were run between samples, and analytical sequences were ordered from low to high Hg to limit carry-over.

2.5. Hair stable carbon, nitrogen and oxygen isotope analysis

Cleaned hair aliquots of 0.50–0.60 mg were analysed for $\delta^{13}C$, $\delta^{15}N$, and $\delta^{18}O$ at the EASIER facility (National Biodiversity Future Center, University of Siena, Italy), using an elemental analyser (FlashSmart EA IsoLink, Thermo Scientific, Germany) interfaced through a ConFlo IV to an isotope ratio mass spectrometer (Delta Q, Thermo Scientific, Germany).

For $\delta^{13}C$ and $\delta^{15}N$, combustion was carried out under helium flow with controlled O_2 addition. Results are expressed relative to Vienna Pee Dee Belemnite (VPDB) for $\delta^{13}C$ and atmospheric nitrogen (AIR) for $\delta^{15}N$. Three international reference materials (USGS-40, USGS-41a, IAEA-61), inserted as unknowns after every fifth study sample, were used for scale normalisation.

For $\delta^{18}O$, the hair aliquots were pyrolyzed in a high-temperature nickel-carbon reactor (1080 °C) with continuous He flow to generate CO for isotopic analysis. Values are reported on the VSMOW-SLAP scale, calibrated by three-point linear regression relative to certified reference materials (IAEA-602, IAEA-600, USGS-54) along in-house cellulose and benzoic acid standards (Coplen and Qi, 2012).

Linearity of the instrumental and stability over the mass range were checked using reference materials, acetanilide (Elemental Microanalysis B2130) and urea (B2904). Bracketing standards showed analytical precision of ± 0.3‰ for $\delta^{13}C$-$\delta^{15}N$ and ± 0.5‰ for $\delta^{18}O$; all samples were run in duplicate, with duplication being within these bounds. Methods were based on established archaeological EA-IRMS best practice (Coplen and Qi, 2012; Meier-Augenstein, 2017; Väre and Nordfors, 2025).

2.6. Data processing and statistical analysis

Normality was assessed with the Kolmogorov-Smirnov under Lilliefors correction, and homogeneity of variances with Levene's test. Descriptive statistics summarised the distribution of THg, $\delta^{13}C$, $\delta^{15}N$ and $\delta^{18}O$. Bivariate associations between hair THg and each isotopic variable were first screened with Pearson correlations. To assess the joint contribution of the isotopic predictors, THg was then modelled with a multivariable generalised linear model (Gamma family, log link) including $\delta^{13}C$, $\delta^{15}N$ and $\delta^{18}O$ as simultaneous predictors; collinearity was evaluated through variance inflation factors. Model robustness was examined with leverage and Cook's distance, and the focal $\delta^{13}C$-THg association was re-tested under a leave-one-out sensitivity analysis. The model code is provided as Supplementary Script S1. All analyses were carried out in R (version 4.4.1; R Core Team, 2024).

3. Results and discussion

3.1. Characterization of the burial sediments

Elemental composition and diagnostic ratios of the three sediment facies identified in the grave backfill are reported in Table S1 and Fig. 2. The facies differ markedly in trace-metal loading: the general fill (Sed1) is metalliferous (elevated Zn, Cu, Pb, Sn, Hg), the Hg^0-bearing facies (Sed3) carries the highest Hg, whereas the near-corpse facies (Sed2), from which the analysed hair was recovered, is the lowest-Hg, clean sand–silt matrix (Fig. 2A). The immediate burial microenvironment of the hair was therefore the facies least enriched in Hg, spatially distinct from the droplet-bearing deposit. The dead were buried in sand-rich backfill with little humic content. The settlement of the pit over time probably permitted secondary deposition of refuses which may have included contaminated industrial waste from a close source. The recovery by the excavators of historical medications stored in waxen globules is at the origin of the droplets of free metallic mercury (Hg^0) found in burial sediments. In early modern Europe, Hg was a mainstay of medical practice, prescribed chiefly for syphilis and for skin conditions such as pediculosis and scabies, and administered as inunctions, fumigations, and oral pills or globules containing metallic mercury or mercurial salts (Apelbaum, 2021; Fornaciari et al., 2011). Nuremberg had a long-regulated apothecary tradition: the Dispensatorium of Valerius Cordus, issued in the city in 1546 and given legal force there, was the first officially recognised pharmacopoeia in Germany and was reissued through the seventeenth century (Urdang, 1951).

Sed1 (general fill) has a metalliferous character with high Zn, Cu, Pb, Sn, and Hg content, high Fe-Mn, low Ca, and moderate Si-Al (Table S1). This geochemical signature suggests mixed urban craft backfill characterized by non-ferrous metalworking waste and brass working refuse with some ferrous slag added during post-subsidence infilling. A little Ca enrichment and small numbers of mortar fragments reflect the lime-rich rubble and ash added used in sanitary capping, as it was common in early modern crisis-burial practices (Antoine, 2008). This metal-rich substrate, with high groundwater levels, is probably at the origin of keratin preservation.

Sed2 (near-corpse deposits) displays the largest partial siliciclastic signal (Si/Al; Fig. 2C), which was due to the clean sand-silt matrix that mitigated trace metal concentrations in the sediments occurring around the bodies. By contrast, Sed3 (Hg^0-bearing sediment) is enriched in calcareous-phosphatic material (high Ca/P and Sr; Fig. 2B-C, Table S1), characteristic of slaked lime, bone phosphate, and mortar debris. The presence of bovine bone fragments in this layer supports the conclusion that quicklime and/or animal bone ash were added on top of cadavers for their decomposition and disinfection. The highest total Hg concentrations found in Sed3 (Fig. 2A), the presence of calcareous-phosphatic

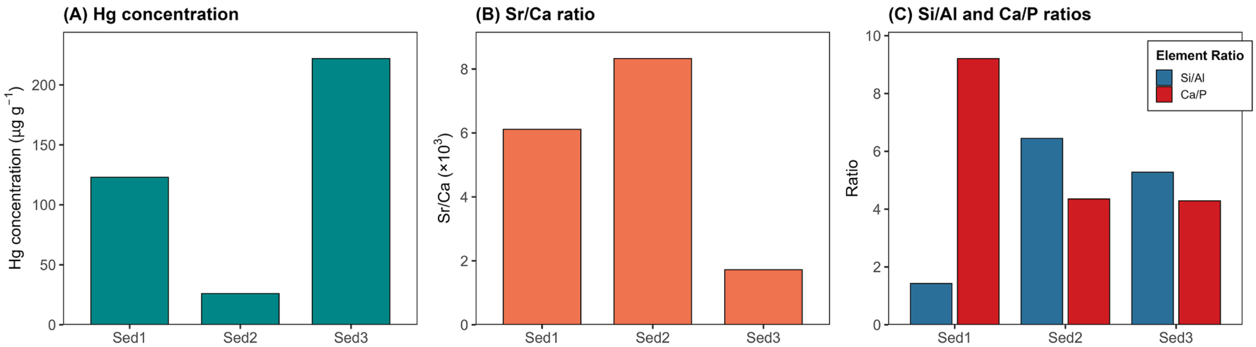

Fig. 2. Mercury concentration and diagnostic element ratios in burial sediments from the Nuremberg mass grave. Three-panel bar plots show (A) total Hg (μg g^{-1}, dry weight), (B) Sr/Ca (× 10^3) ratio, and (C) Si/Al and Ca/P ratios for three facies: Sed1 = general fill, Sed2 = near corpses, and Sed3 = Hg^0-bearing.

enrichment, suggest some level of emergency burial involving disinfecting actions combined with urban refuse filling (Antoine, 2008). This varied post-mortem burial environment might suggest numerous Hg inputs such as anthropogenic material, and potential post-burial exchange as observed in other archaeological hair studies (Zvereva et al., 2017).

We note that the presence of Hg^0 droplets in Sed3 may suggest the grave fill served as a local source Hg, resulting in steep microscale contamination gradients. Similar soil profiling around medieval Danish human skeletons demonstrates that the distribution of Hg released from decaying organic material during burial remains localized, with a pronounced decline in concentration away from large bones, suggestive of rapid immobilization due to adsorption/precipitation within tissue-soil matrix (Rasmussen et al., 2013). Recent multivariate modelling of paired datasets of bone and grave-soil has demonstrated that buried bodies can be Hg sources to their own surrounding sediments, with only a limited additional role for sediment composition other than the presence or absence of Hg-rich minerals (Álvarez-Fernández et al., 2022). The micro-analytical evidence suggests long-term burial may facilitate uptake of exogenous Hg and distal enrichment in hair shafts of archaeological samples (Zvereva et al., 2017). The results emphasize the importance of concurrent consideration of burial-sediment chemistry when assessing hair THg and decontamination as part of ante-mortem exposure reconstruction.

Before hair THg can be read as a record of ante-mortem exposure, the potential for post-burial Hg uptake must be weighed, given the localised Hg^0 droplets in the grave fill. Three lines of evidence constrain this risk. First, the analysed hair derived from the near-corpse facies (Sed2), the lowest-Hg, clean sand–silt matrix (Fig. 2A), spatially distinct from the Hg^0-bearing Sed3; the immediate microenvironment of the strands was therefore not the droplet-bearing deposit. Second, the paired experiment (Section 2.4.1) showed that detergent-solvent treatment removed a median of 86.5% of THg (range 12.6–95.2%; n = 7); dry-brushed and washed aliquots were uncorrelated (Spearman $\rho = -0.21$, $p = 0.65$), so that residual washed THg was independent of the pre-cleaning contamination load (Table S3). Third, hair THg was not associated with keratin-degradation indicators (C/N, N%) once the single specimen with C/N above the well-preserved range was excluded (individual 4, C/N = 4.64; THg-C/N $r = 0.39$, $p = 0.17$ for the remaining individuals), arguing against a diagenetic control on the bulk of the dataset. We nonetheless acknowledge that detergent-solvent washing removes surface-adsorbed and particulate Hg but cannot be assumed to strip Hg^0 bound strongly to keratin sulfhydryl groups; residual exogenous Hg cannot be fully excluded. Accordingly, the reported THg range (0.51–3.38 μg g^{-1}) is interpreted as a conservative upper bound on ante-mortem exposure, and individual 4 is treated with particular caution in Section 3.4.

3.2. *Variability in hair mercury concentrations and inter-individual differences*

THg concentrations in hair varied from 0.51 to 3.38 μg g^{-1} (mean ± SD: 1.81 ± 0.86 μg g^{-1}; n = 15; Fig. 3). The distribution was positively skewed (skewness = 0.45) and very dispersed (CV = 47.7%) reflecting pronounced inter-individual variability. With respect to established hair-Hg reference levels, the Nuremberg concentrations appear elevated. These reference levels are guidance values derived from epidemiological MeHg dose-response relationships, chiefly developmental neurotoxicity endpoints, and serve as screening benchmarks rather than thresholds of acute or cumulative toxicity. Twelve of the 15 individuals (80%) exceeded 1.0 μg g^{-1}, the hair concentration equivalent to the USEPA methylmercury reference dose (Castaño et al., 2015), and four (26.7%) exceeded the JECFA/WHO provisional guidance value of 2.3 μg g^{-1} (UNEP/WHO, 2008). As these values were established for living populations and developmental endpoints, we use them here only as a comparative frame of reference and not to infer health effects in this archaeological sample.

Summary of modern and global reference datasets are presented in Table S2. The centiles calculated in human biomonitoring studies are marked lower than Nuremberg central tendencies. In the large-scale European biomonitoring project DEMOCOPHES, geometric mean hair THg level is at 0.14 μg g^{-1} for children and 0.23 μg g^{-1} for mothers (Castaño et al., 2015; Domínguez-Morueco et al., 2022), with a number of national median values at or below 0.2–0.3 μg g^{-1}. Higher values appear in cohorts with high seafood consumption (e.g., median 1.2 μg g^{-1} in Gulf of Trieste residents; Cegolon et al., 2022), while some fish-industry subgroups reach average concentrations of several μg g^{-1} (e.g., Marano Lagunare; Cegolon et al., 2025). The median in Nuremberg (1.63 μg g^{-1}) is 2–3 times higher than the European background levels and is close to the EFSA-derived hair guidance value of 1.9 μg g^{-1} (EFSA, 2012), representing an intermediate exposure at the global scale. Concentrations are far from those observed in high-exposure riverine and artisanal gold-mining towns in South America, where the central values are at 6–8 μg g^{-1} (e.g., Amazonian communities; Canela et al., 2024; Esplugas et al., 2025), but with many sites much higher. Therefore, the distribution at Nuremberg appears high compared to European reference populations but still lower than the most-affected contemporary populations.

These concentrations should be interpreted primarily as a measure of exposure rather than of effect. This is because the values represent total Hg of unknown speciation in a deceased assemblage, and the reference levels against which they are compared were developed for living populations. With this caveat, the Nuremberg concentrations exceed the levels denoting negligible risk yet remain well below those associated with manifest clinical mercury toxicity. Their potential biological significance, including a possible interaction with nutritional stress and epidemic mortality, is examined in Section 3.5.

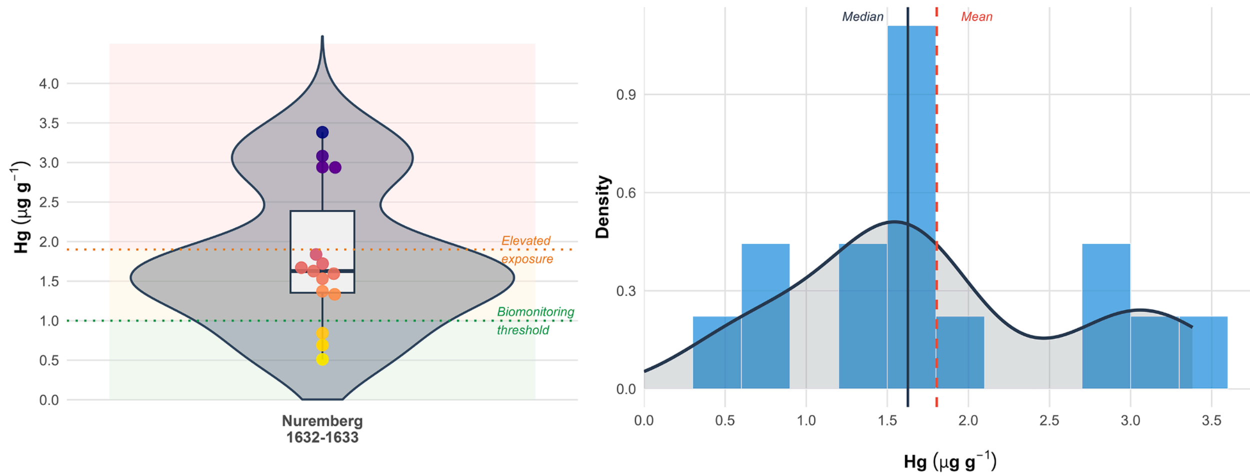

Fig. 3. Hair THg concentrations in Nuremberg mass grave samples. Left, violin plot with individual data points of hair Hg and corresponding box plot together with reference thresholds lines (1.0 μg g^{-1} green line, "Biomonitoring threshold" hair level equivalent to the USEPA MeHg reference dose; Castaño et al., 2015) and exposure above this concentration (EFSA-derived guidance value = 1.9 μg g^{-1} orange line "Elevated exposure"; EFSA, 2012). Right, frequency distribution with kernel density overlay.

3.3. Hair isotopic composition and inferred dietary and physiological patterns

Stable isotope analysis of bulk hair resulted in fairly consistent δ^{13}C values across samples (median −20.724‰; range −22.869 to −20.246‰, VPDB) and generally high δ^{15}N values (median 10.336‰; range 9.954–11.603‰, AIR). δ^{18}O values (median 17.60‰; range 15.975–18.985‰, VSMOW; Fig. 4) were relatively high with low coefficients of variation (2.9–4.8%), indicating homogeneous dietary and hydrological regimes within this population (Bleasdale et al., 2019; Hakenbeck et al., 2010).

Elemental composition analysis resulted in C contents varying from 41.8 to 47.8% (median 44.8%), N contents from 9.0 to 14.4% (median 13.0%), with the C/N ratios ranging from 3.18 to 4.64 (median 3.47). For most samples (66.7%) C/N ratios fell within the expected range for well-preserved keratin (3.0–3.8; Knudson et al., 2015; Nash et al., 2009; O'Connell and Hedges, 1999). A single individual had an elevated ratio (4.64), which might suggest minor diagenetic alteration or a matrix effect. The greater variability observed in N than in C (CV = 9.5% vs 3.9%), possibly reflect an increased diagenetic susceptibility of N-bearing amino acids and metabolic differences during terminal hair growth. Since it is known that physiological stress can alter these metrics the content of C and N, as well as C/N ratio are considered indicators of sample quality rather than proxies of the diet in life (Gutiérrez et al., 2024; Pedergnana et al., 2025).

3.3.1. Dietary baseline and physiological stress

Median hair δ^{15}N (10.3‰) is at the higher end of adult bone-collagen values for early medieval Bavaria (mean 9–10‰; Hakenbeck et al., 2010), suggesting that a locally similar diet heavily reliant on terrestrial resources. The higher δ^{15}N values would be in accord with catabolic nitrogen fractionation during terminal illness, when breakdown of endogenous protein increases ^{15}N enrichment by 1–3‰ at the tissue level owing to preferential excretion of waste ^{14}N-enrichement or so above local food webs; often this is associated with stable or slightly depleted δ^{13}C that may reflect lipid use (Neuberger et al., 2013; Walter et al., 2020). This interpretation is grounded in clinical and experimental observations: hair δ^{15}N rises during sustained negative nitrogen balance and is inversely related to body mass index in starvation and anorexia nervosa, reflecting the recycling of ^{15}N-enriched endogenous protein over weeks to months (Fuller et al., 2004; Hatch et al., 2006; Mekota et al., 2006).

The low inter-individual δ^{15}N variability (CV = 3.9%) does not support the marked socioeconomic differentiation in protein access within this epidemic assemblage, though fine-scale distinctions cannot be ruled out. The δ^{13}C values does not indicate any significant contributions of marine food resources to the diet but they are rather consistent with a diet characterized by mixed terrestrial and freshwater resource. On the basis of the isotopic data, the individuals of Nuremberg mass grave could have consumed freshwater fish as supplementary protein source but this contribution cannot be quantified using bulk isotopic data alone, because of the overlap between C3 terrestrial and temperate freshwater systems (δ^{13}C typically −25 to −20‰; Pedergnana et al., 2025).

Such pattern of uniformly high values of δ^{15}N may be explained by nutritional stress, immune dysregulation and catabolic wasting during epidemic and famine mortality, as reported in previous bioarchaeological studies (DeWitte et al., 2025; Walter et al., 2020). Therefore, the isotopic and elemental data of this study suggests that an essentially terrestrial C3-based diet (with variable animal protein) was consumed by the victims of the plague of Nuremberg during their last few months of life when terminal metabolic stress associated with morbidity came into play.

Elevated δ^{15}N is not, however, diagnostic of catabolism on its own, and three alternatives merit consideration. First, higher intake of animal protein, particularly ^{15}N-enriched freshwater fish, would raise δ^{15}N independently of metabolic state; bulk δ^{15}N cannot separate trophic from catabolic enrichment, and the negative δ^{13}C-δ^{15}N relationship is equally compatible with a freshwater-resource axis (Section 3.4). Second, individual physiological variation cannot be excluded, although the low inter-individual dispersion (CV = 3.9%) indicates a population-wide rather than individual signal. Third, diagenetic alteration is unlikely to drive the pattern: once the single specimen with degraded keratin is excluded (individual 4, C/N = 4.64), δ^{15}N is unrelated to keratin-quality indicators (δ^{15}N-C/N $r = -0.21$, $p = 0.47$; δ^{15}N-N% $r = -0.13$, $p = 0.66$), so that for the well-preserved specimens the enrichment is most plausibly biogenic. We lack independent individual-level evidence, such as systematically scored skeletal stress markers, to confirm catabolism; the documented famine and wartime mortality of 1632–1634 (Alfani and Murphy, 2017) provides plausible population-level context but not direct proof. Compound-specific amino-acid δ^{15}N analysis (e.g., the phenylalanine-glutamic acid offset) would be required to distinguish nutritional stress from protein-source effects (Section 3.3.3). We therefore present catabolic ^{15}N enrichment as one plausible contributor rather than the established cause.

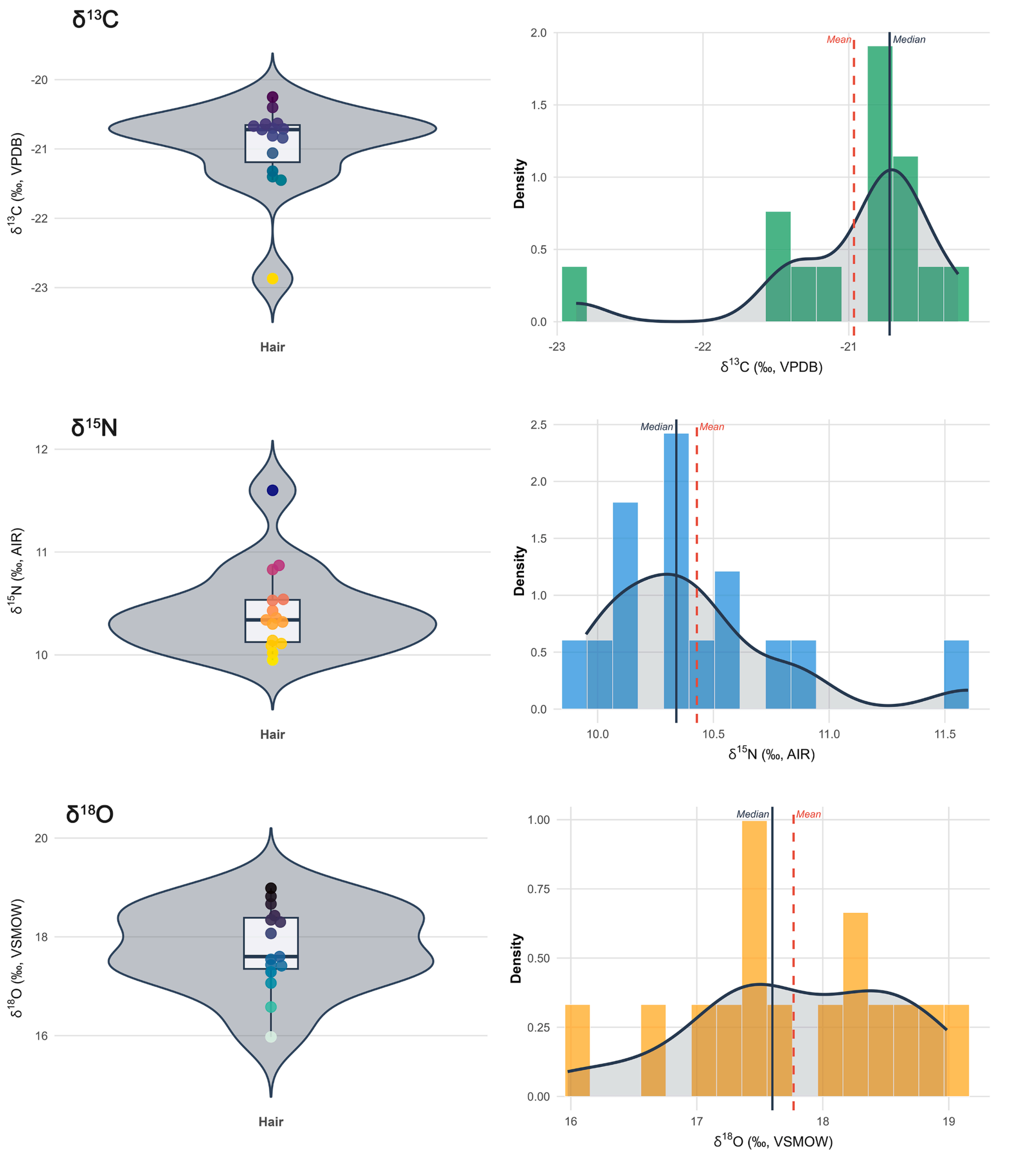

Fig. 4. Stable isotope ratios (δ^{13}C ‰; VPDB; δ^{15}N ‰, AIR; δ^{18}O ‰, VSMOW) in bulk hair from Nuremberg plague victims. Left: violin and box plots with individual data points ($n = 15$, color by value); box = IQR, line = median, whiskers = 1.5 × IQR. Right: frequency distributions with kernel density overlays; median (solid line) and mean (dashed lines).

3.3.2. Sources of drinking water and individual mobility

Hair δ^{18}O represents the isotopic composition of ingested water, and hence as an indicator for drinking-water sources and geolocation. The resulting distribution (median 17.60‰, total range 3.0‰) exhibited low dispersion, no statistical outliers and had a unimodal appearance (Fig. 4), suggesting a common drinking-water supply during the months before death. Hair δ^{18}O integrates several inputs beyond geographic water source, local precipitation δ^{18}O, the type of drinking water (well, river, or rainwater), the water content of food, and metabolic fractionation, so a narrow range constrains, but does not by itself demonstrate, geographic homogeneity. As regional context, groundwater δ^{18}O across south-east Germany is relatively homogeneous (regional range: −12.9 to −6.8‰ VSMOW; mean = −9.6‰), and the Nuremberg/Main River cluster sits at the less-negative end (mean = −9.0‰, −10.6 to −7.7‰ VSMOW (Gaillard et al., 2025); within a single urban catchment, drinking-water δ^{18}O, and hence hair δ^{18}O would be expected to vary little. Consistent with our decision not to perform formal geographic assignment (Section 3.3.3), these values are used only as hydrological background, and ingested water is not back-calculated from hair δ^{18}O. Contemporary populations from temperate regions generally show hair δ^{18}O values that ranges of 2–3‰ within the same city, similar to Nuremberg population (Gautam et al., 2020; Reynard et al., 2016), whose absolute values are towards or just above the enriched end of global ranges (Ehleringer et al., 2008; Reynard et al., 2016).

The very little variability among the individuals indicates exposure to similar isotopic water during their last months. The δ^{18}O in mean hair values can mainly differentiate among residents of contrasting meteoric-water isoscapes to the order of 1 - 2‰, since intra-city variation, seasonal effects, and individual practices (stored water, beer, wine) strongly modulate fine spatial differences between places (Bataille et al., 2022; Gautam et al., 2020; Kennedy et al., 2011; Reynard et al., 2016). The ~3‰ range is consistent with a substantial common hydrological regime characteristic of single urban catchment (Reynard et al., 2016).

The δ^{18}O data show that individuals frequented similar water sources during the months prior to death, offering no evidence of long-range migrants from significantly different climatic zones. In this sample, oxygen-isotopes support the interpretation of a predominantly local urban group that is otherwise based on diet (δ^{13}C-δ^{15}N) and archaeological context.

3.3.3. Methodological considerations

Our interpretations are based on bulk isotopic data whose intrinsic limitations need to be taken into account. For this reason, we did not attempt to back calculate δ^{18}O values in hair into predicted drinking-water or perform formal geographic assignments, for two principal reasons: *i)* it is known that there are inter-laboratory differences that would make direct comparisons with modern isoscapes challenging (Bataille et al., 2022; Coplen and Qi, 2012; Magozzi et al., 2021); *ii)* the applicability of existing frameworks that rely on contemporary water-supply networks might not be representative for 17th-century Nuremberg's preference for cisterns, shallow wells, and evaporatively enriched beverages as common sources of water (Bataille et al., 2022; Kennedy et al., 2011; Reynard et al., 2016).

Fine-scale incremental hair sampling, which was not possible in our study, would be an important advance for mapping temporal trends in isotopic ratios, essential to for a definitive assessment of dietary and physiological contributions to δ^{15}N enrichment (Neuberger et al., 2013). Likewise, compound-specific amino acid analysis (δ^{15}N-AA) would be beneficial to separate trophic from baseline signals (Styring et al., 2015, 2010) and would help to establish pre-terminal dietary baselines by comparing tissues of varying turnover rates (Pedergnana et al., 2025). The application of other proxies, in particular δ^{34}S and proteomic analysis of dietary proteins from dental calculus, could add important information to δ^{13}C-δ^{15}N data, helping refining isotopic characterization of different freshwater dietary sources (Pedergnana et al., 2025). These data would be very useful against simplistic inferences separating the dietary signal from metabolic noise, expected when considering bulk isotopic values for terminal phase individuals (O'Connell, 2025).

3.4. Isotopic correlates of hair mercury

Hair THg was regressed simultaneously on δ^{13}C, δ^{15}N and δ^{18}O in a multivariable generalised linear model (Gamma family, log link; $n = 15$; Supplementary Script S1). δ^{13}C emerged as the sole significant term ($\beta = -0.55$, $p = 0.035$); neither δ^{15}N ($p = 0.27$) nor δ^{18}O ($p = 0.52$) contributed. The model accounted for approximately 30% of the deviance, and variance inflation factors (1.05–1.83) confirmed the absence of problematic collinearity notwithstanding the moderate δ^{13}C-δ^{15}N correlation. Consistent with the model, bivariate analysis showed that THg was negatively correlated with δ^{13}C (Pearson $r = -0.563$, $p = 0.029$, $R^2 = 0.317$) but not with δ^{15}N ($r = 0.206$, $p = 0.462$) or δ^{18}O ($r = -0.144$, $p = 0.610$; Fig. 5), with more ^{13}C-depleted individuals tending towards higher Hg concentrations.

This δ^{13}C-THg association depends on a single observation. Individual 4 combined the most ^{13}C-depleted value (−22.9‰, about 1.4‰ below any other individual) with the highest THg (3.38 μg g^{-1}), giving it disproportionate influence (leverage = 0.82; Cook's distance = 1.33, above the conventional threshold of 1). In a leave-one-out analysis the correlation lost significance only when this individual was removed ($r = -0.32$, $p = 0.26$), whereas excluding any other individual left it essentially unchanged ($r = -0.53$ to -0.67, all $p < 0.05$); equivalently, removing the highest-THg individual renders it non-significant, while removing the lowest-THg individual did not. The δ^{13}C-THg trend is therefore detectable at this sample size but rests entirely on one influential specimen, and we treat it as an exploratory trend rather than as evidence of a dietary control on Hg accumulation.

The most noteworthy aspect of this study is the weak association between hair THg burden and dietary proxies. Inter-individual THg variability was large, whereas δ^{13}C, δ^{15}N and δ^{18}O values were narrowly distributed. Thus, despite relatively uniform isotopic evidence for diet and water source, Hg concentrations differed substantially among individuals. Neither δ^{15}N nor δ^{18}O showed a significant correlation with THg, suggesting that trophic level and drinking-water/geographic signals were not detectable primary predictors of Hg burden in this dataset.

The only possible dietary signal, the exploratory δ^{13}C-Hg trend, relies heavily on one individual with unusually ^{13}C-depleted tissue and low THg concentrations, and cannot by itself support source attribution. If reliable, this pattern could be consistent with freshwater-fish consumption in some individuals, because freshwater food webs in northern

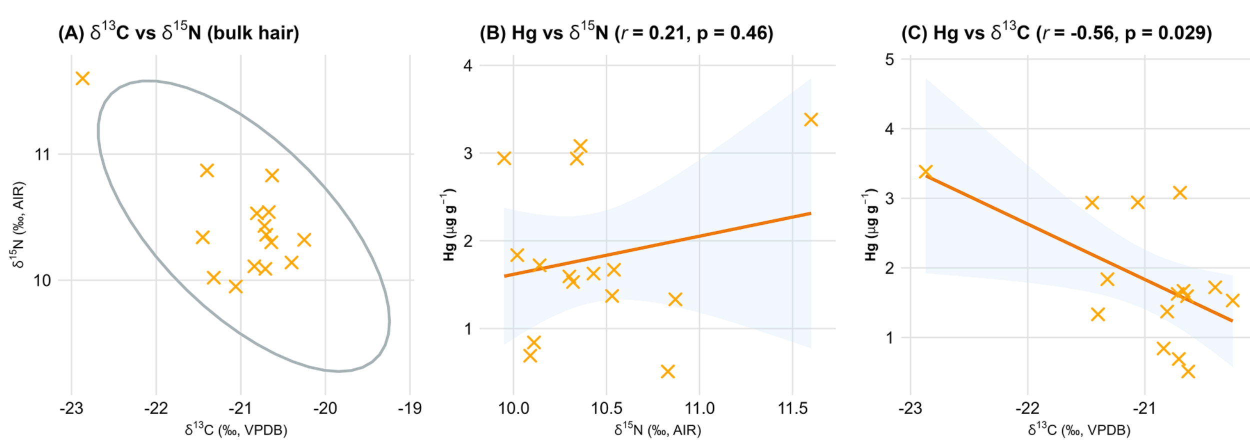

Fig. 5. Correlations of stable isotopes ratios and Hg concentrations in bulk hair. (A) Biplot of δ^{13}C (‰, VPDB) versus δ^{15}N (‰, AIR) with standard ellipse area. (B) Hg (μg g^{-1}) versus δ^{13}C (‰, VPDB) with linear regression and 95% confidence interval. (C) Hg and δ^{15}N with linear regression and 95% confidence interval.

Europe may be ^{13}C-depleted relative to terrestrial C3 resources. However, δ^{13}C alone cannot unambiguously track fish consumption, as values vary geographically and temporally in freshwater consumers, and no historical isotopic baseline is available for the Pegnitz. River sediments can support microbial Hg methylation and MeHg biomagnifies through aquatic food webs (Liu et al., 2025; Veselý et al., 2023). Therefore, riverine foods cannot be ruled out as a dietary Hg source in early modern Nuremberg.

While we do not dismiss a dietary contribution, the data indicate that diet alone cannot explain the observed variation in hair THg concentrations, suggesting additional non-dietary exposure routes, such as Hg-based treatments or occupational exposure (Emslie et al., 2019; Fornaciari et al., 2011). Because only THg was quantified, without speciation or Hg stable-isotope source-apportionment analysis, the relative contributions of dietary and non-dietary routes cannot be resolved; the mixed-exposure scenario therefore remains a hypothesis rather than a demonstrated attribution.

Non-dietary sources warrant equal consideration. Medicinal and occupational Hg exposure (gilding, felt manufacture, cinnabar roasting) were widespread and could have increased Hg intake independently of diet (Emslie et al., 2019; Fornaciari et al., 2011); such exposures would not be expected to positively associate with δ^{13}C unless Hg use co-varied with socioeconomic status that influenced fish access as well; a possible correlate but we are unable to test with current data. The large inter-individual THg variability (CV = 47.7%) contrasts sharply with the narrow stable isotope distributions (δ^{13}C: 2.9%; δ^{15}N: 3.9%, δ^{18}O: 4.8%), indicating that Hg exposure, at least partially, was decoupled from bulk dietary composition and was likely governed by source-specific behaviours not captured in isotope space.

The negative correlation between δ^{13}C and δ^{15}N ($r = -0.654$, $p = 0.008$; Fig. 5A) indicates that individuals with more ^{13}C-depleted values tended to have higher δ^{15}N. This pattern may have two possible explanations. First, it could reflect some contribution of freshwater foods, which can be relatively ^{13}C-depleted and variable in δ^{15}N. Second, it could reflect physiological effects of nutritional stress, which may increase δ^{15}N while lowering δ^{13}C (Styring et al., 2015). In contrast, THg was not related to δ^{18}O, suggesting that differences in drinking water source or geographic origin were not major drivers of Hg burden. Inter-individual Hg variability therefore more likely reflects local exposure routes, such as medical or occupational sources, within a broadly shared urban setting, rather than access to isotopically distinct water sources. However, because the sample size is small ($n = 15$) and preservation-selected, and only total Hg was measured, statistical power is limited, selection effects cannot be excluded and THg alone cannot distinguish dietary from non-dietary exposure.

3.5. *Mercury exposure, malnutrition, and plague deaths: a syndemic approach*

The Nuremberg hair data illustrate that Hg exposure was significantly elevated relative to current European backgrounds and also placed on top of a relatively uniform dietary/hydrological urban background. This leads to the question of whether endemic Hg burden also interacted with plague infection in shaping mortality risk, that is, a syndemic scenario where chemical/nutritional stressors act together with infectious ones as predisposing a more severe disease/mortality. A correct interpretation of this scenario requires comparing the measured exposure to the established range of Hg health effects, which differ depending on the chemical form, dose and duration of the exposure. Methylmercury, the form found in food, is primarily a neurotoxin. High doses of this compound cause sensory loss, ataxia and visual impairment characteristic of Minamata disease (WHO, 1990), whereas developmental neurotoxicity (which informs modern guidelines) has been observed in maternal hair mercury at concentrations of about 10 μg g^{-1} (EFSA, 2012). Exposure to elemental or inorganic Hg, the species relevant to early modern medical and occupational practices, can cause kidney disease, tremor and a neurobehavioral disorder called erethism; excessive exposure also results in gingivostomatitis (Kobal et al., 2017; WHO, 1991). The Nuremberg concentrations of 0.51–3.38 μg g^{-1} are well below the thresholds needed to cause overt clinical effects and are within the low-to-moderate levels associated with documented subclinical neurological effects.

Set against this context (Table 1), the Nuremberg hair THg values (0.51–3.38 μg g^{-1}; 80% above the USEPA 1.0 μg g^{-1} reference and four individuals above the JECFA/WHO 2.3 μg g^{-1} guidance) exceed contemporary European biomonitoring hair Hg (DEMOCOPHES/HBM4EU geometric means of 0.1–0.23 μg g^{-1}; (Castaño et al., 2015; Domínguez-Morueco et al., 2022), and are comparable to or above the higher central values (1.2–1.9 μg g^{-1}) reported for higher-seafood European coastal adults (Trieste, median = 1.2; Spanish adult women, geometric mean = 1.87; (Castaño et al., 2019; Cegolon et al., 2022) while remaining far below the extreme values reported for archaeological hair subject to documented topical mercurial treatment (827 μg g^{-1}; Fornaciari et al., 2011) or exogenous burial uptake (up to 1100 μg g^{-1}; Zvereva et al., 2017). Archaeological bone Hg from medieval Europe spans background levels to several μg g^{-1} in mercury-treated individuals (Álvarez-Fernández et al., 2022; Rasmussen et al., 2013) but is not directly comparable to hair.

At such concentrations, the consequences most relevant to an epidemic context are immunological. Experimental and epidemiological evidence indicates that chronic low-to-moderate Hg exposure can perturb immune function by altering lymphocyte proliferation, cytokine balance, and oxidative stress pathways, and thereby modulate host susceptibility to infection independently of overt toxicity (Wu et al., 2024). Consistent with this, gold-mining communities in the Brazilian Amazon with hair Hg of 0.3–83.2 μg g^{-1} showed a 4.2-fold higher prevalence of malaria than non-exposed neighbours (Crompton et al., 2002). Although exposure at Nuremberg was lower, the upper tail of the distribution falls within a range where subclinical immunomodulation is plausible, particularly when undernutrition or co-infections coexisted with sustained Hg exposure.

In an early modern urban scenario, more than one route to Hg exposure can be hypothesized. The ways people could be exposed to repeated Hg handling and inhalation included medical preparations prescribed for lice, scabies, and venereal disease as well as occupational activities such as gilding, felt production and mirror manufacture (Emslie et al., 2019; Fornaciari et al., 2011). Due to the wide range of exposure conditions, it is reasonable to assume that the adverse effects of Hg exposure were unevenly distributed in the population in relation to several societal factors such as status, wartime disruption or changing food security condition (Alfani and Murphy, 2017). This may have played a role in modulating the epidemic mortality in line with earlier bioarchaeological studies that have demonstrated that individuals with skeletal or isotopic markers of chronic stress were disproportionately likely to die during outbreaks (DeWitte et al., 2025; DeWitte and Wood, 2008; Walter et al., 2020).

Our data suggest that chronic Hg exposure and nutritional stress may have contributed to increase susceptibility to *Yersinia pestis* infection and/or to aggravating disease and death, in at least a portion of the infected individuals. Given the sample size and the absence of non-plague comparative material, this scenario is offered as hypothesis to be tested rather than as demonstrated property of the buried population. It nonetheless provides a framework for combining trace metal burdens with stable isotope evidence to examine how overlapping stressors may have shaped epidemic mortality in early modern period.

4. Conclusions

The analysis of archaeological scalp hair from the Nuremberg plague mass grave provided a useful framework to infer Hg exposure in an urban population of in pre-modern times. THg concentrations and δ^{13}C-δ^{15}N, and δ^{18}O signatures indicated homogeneous terrestrial C3-based

Table 1
Hair and bone total mercury (THg) in the Nuremberg series compared with selected archaeological and modern reference datasets. Hair and bone Hg are not directly comparable owing to differences in tissue uptake and retention; bone values are included only as an order-of-magnitude context.

Site / population	Period	Tissue	n	THg (μg g^{-1})	Inferred dominant source	Reference
Nuremberg plague mass grave (this study)	1632–1634 CE	Scalp hair	15	0.51–3.38 (median 1.63)	Mixed	This study
Ferdinand II of Aragon, Naples (Italy)	1496 CE	Scalp hair	1	827	Topical anti-lice mercurial	Fornaciari et al., 2011
Xiongnu nobility, Noin-Ula (Mongolia)	1st century BCE- 1st century CE	Hair	41	up to ~1100	Exogenous (burial uptake)	Zvereva et al., 2017
Medieval cemeteries, Denmark (Ribe, Horsens)	Medieval	Femoral bone	7	0.05–0.35	Background + therapeutic Hg	Rasmussen et al., 2013
A Lanzada, NW Spain	6th-7th century CE	Bone	73 (samples)	Diagenetically modulated	Diagenesis-influenced	Álvarez-Fernández et al., 2022
Modern European biomonitoring (DEMOCOPHES/HBM4EU)	Present	Hair	>1800	0.1–0.23 (General population); 1.2–1.9 (higher-seafood coastal adults)	Dietary MeHg (seafood)	Castaño et al., 2015; Domínguez-Morueco et al., 2022

diets and water source with a possible effect of catabolic stress in the months preceding death. Exposure to Hg of the analysed Nuremberg specimens, as inferred from hair analysis, appeared consistently higher than contemporary European background levels and overlapping with high-seafood consumer populations of the 21st century. The large inter-individual THg variability against a homogeneous dietary and hydrological background suggests that diet alone did not control Hg burden, a pattern compatible with additional non-dietary routes (therapeutic and occupational exposure). Because no Hg speciation or isotopic source apportionment was performed, the relative contributions of dietary (e.g., freshwater fish) and non-dietary pathways could not be resolved, and source attribution remains exploratory.

These results suggest overlapping stressors likely influenced epidemic mortality. We propose, as a hypothesis for testing in larger assemblages, a syndemic scenario in which chemical (elevated Hg exposure), physiological (enriched $\delta^{15}N$ consistent with catabolic stress) and epidemic (plague infection) factors may have acted together to shape disease risk during the 1632–34 outbreak. Because the analysed series is small ($n = 15$) preservation-selected, and not necessarily representative of a wider population, Hg exposure among plague victims may have differed from that of survivors, the reported associations are exploratory and selection effects cannot be excluded. Comparisons among plague sites, Hg isotopic source apportionment and expanded sampling are needed to test these patterns and evaluate the extent of geographic variability in pre-industrial Hg exposure.

Declarations

All authors have read, understood, and have complied as applicable with the statement on "Ethical responsibilities of Authors" as found in the Instructions for Authors.

Funding

This work was supported by the National Recovery and Resilience Plan (NRRP), project “National Biodiversity Future Center - NBFC” (CN_00000033, CUP B63C22000650007).

CRediT authorship contribution statement

Fabrizio Monaci: Writing – review & editing, Writing – original draft, Visualization, Supervision, Funding acquisition, Formal analysis, Conceptualization. **Riccardo Fedeli:** Writing – review & editing, Resources, Methodology, Investigation, Data curation, Conceptualization. **Kaylie Anne Walsh:** Writing – review & editing, Resources, Methodology, Investigation. **Melanie Langbein:** Writing – review & editing, Resources, Methodology, Investigation. **Julian Decker:** Writing – review & editing, Resources, Methodology, Investigation, Conceptualization.

Declaration of competing interest

The authors declare the following financial interests/personal relationships which may be considered as potential competing interests: Fabrizio Monaci reports financial support was provided by National Biodiversity Future Center - NBFC. If there are other authors, they declare that they have no known competing financial interests or personal relationships that could have appeared to influence the work reported in this paper.

Acknowledgments

The authors are grateful to Gabriele Schiefer of wbg GmbH Nuremberg for her support in facilitating this research. The Article Processing Charge for open access publication was covered by In Terra Veritas GmbH.

Fabrizio Monaci was supported under the National Recovery and Resilience Plan (NRRP), Mission 4 Component 2 Investment 1.4 - Call for tender No. 3138 of 16 December 2021, rectified by Decree n.3175 of 18 December 2021 of Italian Ministry of University and Research funded by the European Union - NextGenerationEU; Award Number: Project code CN_00000033, Concession Decree No. 1034 of 17 June 2022 adopted by the Italian Ministry of University and Re-search, CUP B63C22000650007, Project title “National Biodiversity Future Center - NBFC”.

Supplementary materials

Supplementary material associated with this article can be found, in the online version, at doi:10.1016/j.hazadv.2026.101469.

Data availability

Data will be made available on request.

References

Alfani, G., Murphy, T.E., 2017. Plague and lethal epidemics in the pre-industrial world. J. Econ. Hist. 77, 314–343. https://doi.org/10.1017/S0022050717000092.
Álvarez-Fernández, N., Martínez Cortizas, A., López-Costas, O., 2022. Structural equation modelling of mercury intra-skeletal variability on archaeological human remains. Sci. Total Environ. 851, 158015. https://doi.org/10.1016/j.scitotenv.2022.158015.
Antoine, D., 2008. The archaeology of “plague. Med. Hist. Suppl. 52, 101–114.

Apelbaum, N., 2021. *Doron medicum* —the gift of medicine: how a rare 17th century medical translation positively impacted the community and predicted current analgesic techniques. Anaesth. Intensive Care 49, 41–50. https://doi.org/10.1177/0310057X211038570.
Aranda, P., 2008. Cloud point extraction of mercury with PONPE 7.5 prior to its determination in biological samples by ETAAS. TalantaTalanta 75, 307–311. https://doi.org/10.1016/j.talanta.2007.11.012.
Auerswald, K., Rossmann, A., Schäufele, R., Schwertl, M., Monahan, F.J., Schnyder, H., 2011. Does natural weathering change the stable isotope composition (^{2}H,^{13}C,^{15} N,^{18} O and^{34} S) of cattle hair? Rapid Commun. Mass Spectrom. 25, 3741–3748. https://doi.org/10.1002/rcm.5284.
Bataille, C.P., Ammer, S.T.M., Bhuiyan, S., Chartrand, M.M.G., St-Jean, G., Bowen, G.J., 2022. Multi-isotopes in human hair: a tool to initiate cross-border collaboration in international cold-cases. PLoS. One 17, e0275902. https://doi.org/10.1371/journal.pone.0275902.
Bleasdale, M., Ponce, P., Radini, A., Wilson, A.S., Doherty, S., Daley, P., Brown, C., Spindler, L., Sibun, L., Speller, C., Alexander, M.M., 2019. Multidisciplinary investigations of the diets of two post-medieval populations from London using stable isotopes and microdebris analysis. Archaeol. Anthropol. Sci. 11, 6161–6181. https://doi.org/10.1007/s12520-019-00910-8.
Bowen, G.J., 2010. Isoscapes: spatial pattern in isotopic biogeochemistry. Annu Rev. Earth. Planet. Sci. 38, 161–187. https://doi.org/10.1146/annurev-earth-040809-152429.
Canela, T.A., Monteiro, L.C., Cabral, C.D.S., Ximenes, F.D.S., Oliveira, I.A.D.S., Bernardi, J.V.E., Almeida, R.D., Bastos, W.R., 2024. Mercury in fish and Human hair and estimated dietary intake in a riverside community of the Madeira River Basin in the Brazilian Amazon. Toxics 12, 208. https://doi.org/10.3390/toxics12030208.
Capuzzo, G., Fiorin, E., Beck De Lotto, M.A., Betto, A., Tasca, G., Di Tonto, S., Forlin, P., Snoeck, C., Cheung, C., 2025. Diet, mobility, and life histories during the early medieval period at San Vito al Tagliamento, Italy. J. Archaeol. Sci. Rep. 66, 105328. https://doi.org/10.1016/j.jasrep.2025.105328.
Castaño, A., Cutanda, F., Esteban, M., Pärt, P., Navarro, C., Gómez, S., Rosado, M., López, A., López, E., Exley, K., Schindler, B.K., Govarts, E., Casteleyn, L., Kolossa-Gehring, M., Fiddicke, U., Koch, H., Angerer, J., Hond, E.D., Schoeters, G., Sepai, O., Horvat, M., Knudsen, L.E., Aerts, D., Joas, A., Biot, P., Joas, R., Jiménez-Guerrero, J. A., Diaz, G., Pirard, C., Katsonouri, A., Cerna, M., Gutleb, A.C., Ligocka, D., Reis, F. M., Berglund, M., Lupsa, I.-R., Halzlová, K., Charlier, C., Cullen, E., Hadjipanayis, A., Krsková, A., Jensen, J.F., Nielsen, J.K., Schwedler, G., Wilhelm, M., Rudnai, P., Középesy, S., Davidson, F., Fischer, M.E., Janasik, B., Namorado, S., Gurzau, A.E., Jajcaj, M., Mazej, D., Tratnik, J.S., Larsson, K., Lehmann, A., Crettaz, P., Lavranos, G., Posada, M., 2015. Fish consumption patterns and hair mercury levels in children and their mothers in 17 EU countries. Environ. Res. 141, 58–68. https://doi.org/10.1016/j.envres.2014.10.029.
Castaño, A., Pedraza-Díaz, S., Cañas, A.I., Pérez-Gómez, B., Ramos, J.J., Bartolomé, M., Pärt, P., Soto, E.P., Motas, M., Navarro, C., Calvo, E., Esteban, M., 2019. Mercury levels in blood, urine and hair in a nation-wide sample of Spanish adults. Sci. Total Environ. 670, 262–270. https://doi.org/10.1016/j.scitotenv.2019.03.174.
Cegolon, L., Covelli, S., Patriarca, E., Petranich, E., Floreani, F., Sansone, D., Mastrangelo, G., Larese Filon, F., 2025. Contrasting hair mercury in fishermen and workers of fish industry of Marano Lagunare (Upper Adriatic Sea), a coastal lagoon area contaminated by mining and industrial activities, against residents from the Dolomites Alps. Sci. Total Environ. 965, 178039. https://doi.org/10.1016/j.scitotenv.2024.178039.
Cegolon, L., Petranich, E., Pavoni, E., Floreani, F., Barago, N., Papassissa, E., Larese Filon, F., Covelli, S., 2022. Concentration of mercury in human hair and associated factors in residents of the Gulf of Trieste (North-Eastern Italy). Environ. Sci. Pollut. Res. 30, 21425–21437. https://doi.org/10.1007/s11356-022-23384-z.
Cooke, C.A., Martínez-Cortizas, A., Bindler, R., Sexauer Gustin, M., 2020. Environmental archives of atmospheric Hg deposition – a review. Sci. Total Environ. 709, 134800. https://doi.org/10.1016/j.scitotenv.2019.134800.
Coplen, T.B., Qi, H., 2012. USGS42 and USGS43: human-hair stable hydrogen and oxygen isotopic reference materials and analytical methods for forensic science and implications for published measurement results. Forensic Sci. Int. 214, 135–141. https://doi.org/10.1016/j.forsciint.2011.07.035.
Corella, J.P., Sierra, M.J., Garralón, A., Millán, R., Rodríguez-Alonso, J., Mata, M.P., De Vera, A.V., Moreno, A., González-Sampériz, P., Duval, B., Amouroux, D., Vivez, P., Cuevas, C.A., Adame, J.A., Wilhelm, B., Saiz-Lopez, A., Valero-Garcés, B.L., 2021. Recent and historical pollution legacy in high altitude Lake Marboré (Central Pyrenees): a record of mining and smelting since pre-roman times in the Iberian Peninsula. Sci. Total Environ. 751, 141557. https://doi.org/10.1016/j.scitotenv.2020.141557.
Crompton, P., Ventura, A.M., De Souza, J.M., Santos, E., Strickland, G.T., Silbergeld, E., 2002. Assessment of mercury exposure and malaria in a Brazilian Amazon riverine community. Environ. Res. 90, 69–75. https://doi.org/10.1006/enrs.2002.4358.
DeWitte, S.N., Beaumont, J., Walter, B.S., Towers, J.R., Brennan, E.J., 2025. Childhood nutritional stress and later-life health outcomes in medieval England: evidence from incremental dentine analysis. Sci. Adv. 11, eadw7076.
DeWitte, S.N., Wood, J.W., 2008. Selectivity of black death mortality with respect to preexisting health. Proc. Natl. Acad. Sci. U.S.A. 105, 1436–1441. https://doi.org/10.1073/pnas.0705460105.
Domínguez-Morueco, N., Pedraza-Díaz, S., González-Caballero, M.D.C., Esteban-López, M., De Alba-González, M., Katsonouri, A., Santonen, T., Cañas-Portilla, A., Castaño, A., 2022. Methylmercury risk assessment based on European Human biomonitoring data. Toxics 10, 427. https://doi.org/10.3390/toxics10080427.
Driscoll, C.T., Mason, R.P., Chan, H.M., Jacob, D.J., Pirrone, N., 2013. Mercury as a global pollutant: sources, pathways, and effects. Environ. Sci. Technol. 47, 4967–4983. https://doi.org/10.1021/es305071v.
Du, B., Yin, R., Fu, X., Li, P., Feng, X., Maurice, L., 2021. Use of mercury isotopes to quantify sources of human inorganic mercury exposure and metabolic processes in the human body. Environ. Int. 147, 106336. https://doi.org/10.1016/j.envint.2020.106336.
Eerkens, J.W., Hull, B., Goodman, J., Evoy, A., Kapp, J.D., Hussain, S., Green, R.E., 2017. Stable C and N isotope analysis of hair suggest undernourishment as a factor in the death of a mummified girl from late 19th century San Francisco, CA. PLoS. One 12, e0184921. https://doi.org/10.1371/journal.pone.0184921.
EFSA, 2012. Scientific Opinion on the Risk for Public Health Related to the Presence of Mercury and Methylmercury in Food. EFS2, p. 10. https://doi.org/10.2903/j.efsa.2012.2985.
Ehleringer, J.R., Bowen, G.J., Chesson, L.A., West, A.G., Podlesak, D.W., Cerling, T.E., 2008. Hydrogen and oxygen isotope ratios in human hair are related to geography. Proc. Natl. Acad. Sci. U.S.A. 105, 2788–2793. https://doi.org/10.1073/pnas.0712228105.
Emslie, S.D., Alderman, A., McKenzie, A., Brasso, R., Taylor, A.R., Molina Moreno, M., Cambra-Moo, O., González Martín, A., Silva, A.M., Valera, A., García Sanjuán, L., Vijande Vila, E., 2019. Mercury in archaeological human bone: biogenic or diagenetic? J. Archaeol. Sci. 108, 104969. https://doi.org/10.1016/j.jas.2019.05.005.
Esplugas, J., Neves Cezarette, G., Tessier, E., Barbosa Jr, F., Bueno, M., Pedrero Zayas, Z., 2025. Dynamics of mercury speciation and selenium levels in hair under seasonal and dietary influences in an Amazonian riverside population. J. Hazard. Mater. https://doi.org/10.2139/ssrn.5156906.
Esteban, M., Schindler, B.K., Jiménez, J.A., Koch, H.M., Angerer, J., Rosado, M., Gómez, S., Casteleyn, L., Kolossa-Gehring, M., Becker, K., Bloemen, L., Schoeters, G., Hond, E.D., Sepai, O., Exley, K., Horvat, M., Knudsen, L.E., Joas, A., Joas, R., Aerts, D., Biot, P., Borošová, D., Davidson, F., Dumitrascu, I., Fischer, M.E., Grander, M., Janasik, B., Jones, K., Kašparová, L., Larssen, T., Naray, M., Nielsen, F., Hohenblum, P., Pinto, R., Pirard, C., Plateel, G., Tratnik, J.S., Wittsiepe, J., Castaño, A., 2015. Mercury analysis in hair: comparability and quality assessment within the transnational COPHES/DEMOCOPHES project. Environ. Res. 141, 24–30. https://doi.org/10.1016/j.envres.2014.11.014.
Fedeli, R., Di Lella, L.A., Loppi, S., 2024. Suitability of XRF for routine analysis of multi-elemental composition: a multi-standard verification. MPS. 7, 53. https://doi.org/10.3390/mps7040053.
Fornaciari, G., Marinozzi, S., Gazzaniga, V., Giuffra, V., Picchi, M.S., Giusiani, M., Masetti, M., 2011. The use of mercury against pediculosis in the renaissance: the case of Ferdinand II of Aragon, king of Naples, 1467–96. Med. Hist. 55, 109–115. https://doi.org/10.1017/S0025727300006074.
Fuller, B.T., Fuller, J.L., Sage, N.E., Harris, D.A., O'Connell, T.C., Hedges, R.E.M., 2004. Nitrogen balance and δ^{15} N: why you're not what you eat during pregnancy. Rapid Commun. Mass Spectrom. 18, 2889–2896. https://doi.org/10.1002/rcm.1708.
Gaillard, A., Van Geldern, R., Barth, J.A.C., Stumpp, C., 2025. A new high-resolution groundwater isoscape for south-east Germany: insights from differences in relation to precipitation. Hydrol. Earth. Syst. Sci. 29, 3853–3863. https://doi.org/10.5194/hess-29-3853-2025.
García Gómez, M., Diego Caballero Klink, J., Boffetta, P., Español, S., Sällsten, G., Gómez Quintana, J., 2007. Exposure to mercury in the mine of Almadén. Occup. Environ. Med. 64, 389–395. https://doi.org/10.1136/oem.2006.030940.
Gautam, M.K., Song, B.-Y., Shin, W.-J., Bong, Y.-S., Lee, K.-S., 2020. Spatial variations in oxygen and hydrogen isotopes in waters and human hair across South Korea. Sci. Total Environ. 726, 138365. https://doi.org/10.1016/j.scitotenv.2020.138365.
Gustin, M.S., Bank, M.S., Bishop, K., Bowman, K., Branfireun, B., Chételat, J., Eckley, C. S., Hammerschmidt, C.R., Lamborg, C., Lyman, S., Martínez-Cortizas, A., Sommar, J., Tsui, M.T.-K., Zhang, T., 2020. Mercury biogeochemical cycling: a synthesis of recent scientific advances. Sci. Total Environ. 737, 139619. https://doi.org/10.1016/j.scitotenv.2020.139619.
Gutiérrez, E., Mitchell, S., Hambly, C., Sayle, K.L., Von Kriegsheim, A., Speakman, J.R., Britton, K., 2024. Carbon, nitrogen, and sulfur elemental and isotopic variations in mouse hair and bone collagen during short-term graded calorie restriction. iScience 27, 110059. https://doi.org/10.1016/j.isci.2024.110059.
Hakenbeck, S., McManus, E., Geisler, H., Grupe, G., O'Connell, T., 2010. Diet and mobility in early medieval Bavaria: a study of carbon and nitrogen stable isotopes. Am. J. Phys. Anthropol. 143, 235–249. https://doi.org/10.1002/ajpa.21309.
Hatch, K.A., Crawford, M.A., Kunz, A.W., Thomsen, S.R., Eggett, D.L., Nelson, S.T., Roeder, B.L., 2006. An objective means of diagnosing anorexia nervosa and bulimia nervosa using^{15} N/^{14} N and^{13} C/^{12}C ratios in hair. Rapid Commun. Mass Spectrom. 20, 3367–3373. https://doi.org/10.1002/rcm.2740.
Kennedy, C.D., Bowen, G.J., Ehleringer, J.R., 2011. Temporal variation of oxygen isotope ratios (δ18O) in drinking water: implications for specifying location of origin with human scalp hair. Forensic Sci. Int. 208, 156–166. https://doi.org/10.1016/j.forsciint.2010.11.021.
Knudson, K.J., Peters, A.H., Cagigao, E.T., 2015. Paleodiet in the Paracas Necropolis of Wari Kayan: carbon and nitrogen isotope analysis of keratin samples from the south coast of Peru. J. Archaeol. Sci. 55, 231–243. https://doi.org/10.1016/j.jas.2015.01.011.
Kobal, A.B., Snoj Tratnik, J., Mazej, D., Fajon, V., Gibičar, D., Miklavčič, A., Kocman, D., Kotnik, J., Sešek Briški, A., Osredkar, J., Krsnik, M., Prezelj, M., Knap, Č., Križaj, B., Liang, L., Horvat, M., 2017. Exposure to mercury in susceptible population groups living in the former mercury mining town of Idrija, Slovenia. Environ. Res. 152, 434–445. https://doi.org/10.1016/j.envres.2016.06.037.

Liu, S., Liao, L., Liu, J., Wei, X., 2025. Sediment mercury and methylmercury dynamics during reservoir operation. Sci. Rep. 15, 18011. https://doi.org/10.1038/s41598-025-03255-6.
Lombardi, G., Lanzirotti, A., Qualls, C., Socola, F., Ali, A.-M., Appenzeller, O., 2012. Five hundred years of mercury exposure and adaptation. J. Biomed. Biotechnol. 2012, 1–10. https://doi.org/10.1155/2012/472858.
Lorentz, K.O., De Nolf, W., Cotte, M., Ioannou, G., Foruzanfar, F., Zaruri, M.R., Sajjadi, S. M.S., 2020. Synchrotron radiation micro X-ray fluorescence (SR-μXRF) elemental mapping of ancient hair: metals and health at 3rd millennium BCE Shahr-i Sokhta, Iran. J. Archaeol. Sci. 120, 105193. https://doi.org/10.1016/j.jas.2020.105193.
Macko, S.A., Engel, M.H., Andrusevich, V., Lubec, G., O'Connell, T.C., Hedges, R.E.M., 1999. Documenting the diet in ancient human populations through stable isotope analysis of hair. Phil. Trans. R. Soc. Lond. B 354, 65–76. https://doi.org/10.1098/rstb.1999.0360.
Magozzi, S., Bataille, C.P., Hobson, K.A., Wunder, M.B., Howa, J.D., Contina, A., Vander Zanden, H.B., Bowen, G.J., 2021. Calibration chain transformation improves the comparability of organic hydrogen and oxygen stable isotope data. Methods Ecol. Evol. 12, 732–747. https://doi.org/10.1111/2041-210X.13556.
Martinis, E.M., Wuilloud, R.G., 2010. Cold vapor ionic liquid-assisted headspace single-drop microextraction: a novel preconcentration technique for mercury species determination in complex matrix samples. J. Anal. At. Spectrom. 25, 1432. https://doi.org/10.1039/c004678g.
Martínez-Cortizas, A., Pontevedra-Pombal, X., García-Rodeja, E., Nóvoa-Muñoz, J.C., Shotyk, W., 1999. Mercury in a Spanish peat bog: archive of climate change and atmospheric metal deposition. Science 284, 939–942. https://doi.org/10.1126/science.284.5416.939.
Meier-Augenstein, W., 2017. Stable Isotope Forensics - Methods and Applications of Stable Isotope Analysis, 2nd ed. https://doi.org/10.1002/9781119080190
Mekota, A., Grupe, G., Ufer, S., Cuntz, U., 2006. Serial analysis of stable nitrogen and carbon isotopes in hair: monitoring starvation and recovery phases of patients suffering from anorexia nervosa. Rapid Commun. Mass Spectrom. 20, 1604–1610. https://doi.org/10.1002/rcm.2477.
Morrone, A., Tõrv, M., Piombino-Mascali, D., Saupe, T., Sepp, H., Valk, H., Malve, M., Oras, E., 2023. Children of the grave: investigating non-adult feeding practices in medieval and early modern Estonia through stable isotope analysis. PLoS. One 18, e0279546. https://doi.org/10.1371/journal.pone.0279546.
Nash, S.H., Kristal, A.R., Boyer, B.B., King, I.B., Metzgar, J.S., O'Brien, D.M., 2009. Relation between stable isotope ratios in human red blood cells and hair: implications for using the nitrogen isotope ratio of hair as a biomarker of eicosapentaenoic acid and docosahexaenoic acid. Am. J. Clin. Nutr. 90, 1642–1647. https://doi.org/10.3945/ajcn.2009.28482.
Neuberger, F.M., Jopp, E., Graw, M., Püschel, K., Grupe, G., 2013. Signs of malnutrition and starvation—reconstruction of nutritional life histories by serial isotopic analyses of hair. Forensic Sci. Int. 226, 22–32. https://doi.org/10.1016/j.forsciint.2012.10.037.
O'Brien, D.M., Wooller, M.J., 2007. Tracking human travel using stable oxygen and hydrogen isotope analyses of hair and urine. Rapid Commun. Mass Spectrom. 21, 2422–2430. https://doi.org/10.1002/rcm.3108.
O'Connell, T.C., 2025. The signal and the noise: inherent challenges for isotopic studies in bioarchaeology. J. Archaeol. Sci. 183, 106379. https://doi.org/10.1016/j.jas.2025.106379.
O'Connell, T.C., Hedges, R.E.M., 1999. Investigations into the effect of diet on modern human hair isotopic values. Am. J. Phys. Anthropol. 108, 409–425. https://doi.org/10.1002/(SICI)1096-8644(199904)108:4%3C409::AID-AJPA3%3E3.0.CO;2-E.
Pedergnana, A., Grossmann, J., Turck, R., Goujon, A., Rühli, F., Wilkin, S., Eppenberger, P., Lehn, C., 2025. Reconstructing medieval diets through the integration of stable isotope and proteomic analyses from two European burial sites. Sci. Rep. 15, 26442. https://doi.org/10.1038/s41598-025-10103-0.
Pragst, F., Balikova, M.A., 2006. State of the art in hair analysis for detection of drug and alcohol abuse. Clin. Chim. Acta 370, 17–49. https://doi.org/10.1016/j.cca.2006.02.019.
R Core Team, 2024. R: a Language and Environment for Statistical Computing (manual). R Foundation for Statistical Computing, Vienna, Austria.
Rasmussen, K.L., Skytte, L., Ramseyer, N., Boldsen, J.L., 2013. Mercury in soil surrounding medieval human skeletons. Herit. Sci. 1, 16. https://doi.org/10.1186/2050-7445-1-16.
Reynard, L.M., Burt, N., Koon, H.E.C., Tuross, N., 2016. Limits and possibilities in the geolocation of humans using multiple isotope ratios (H, O, N, C) of hair from east coast cities of the USA. Isotopes. Environ. Health Stud. 52, 498–512. https://doi.org/10.1080/10256016.2016.1143821.
Squires, K., Errickson, D., Márquez-Grant, N. (Eds.), 2019. Ethical Approaches to Human Remains: A Global Challenge in Bioarchaeology and Forensic Anthropology. Springer, Cham.
Streets, D.G., Horowitz, H.M., Jacob, D.J., Lu, Z., Levin, L., Ter Schure, A.F.H., Sunderland, E.M., 2017. Total mercury released to the environment by Human activities. Environ. Sci. Technol. 51, 5969–5977. https://doi.org/10.1021/acs.est.7b00451.
Styring, A.K., Fraser, R.A., Arbogast, R.-M., Halstead, P., Isaakidou, V., Pearson, J.A., Schäfer, M., Triantaphyllou, S., Valamoti, S.M., Wallace, M., Bogaard, A., Evershed, R.P., 2015. Refining human palaeodietary reconstruction using amino acid δ15N values of plants, animals and humans. J. Archaeol. Sci. 53, 504–515. https://doi.org/10.1016/j.jas.2014.11.009.
Styring, A.K., Sealy, J.C., Evershed, R.P., 2010. Resolving the bulk δ15N values of ancient human and animal bone collagen via compound-specific nitrogen isotope analysis of constituent amino acids. Geochim. Cosmochim. Acta 74, 241–251. https://doi.org/10.1016/j.gca.2009.09.022.
UNEP/WHO, 2008. Guidance for Identifying Populations At Risk from Mercury Exposure. World Health Organization, Geneva, Switzerland.
Urdang, G., 1951. The development of pharmacopoeias; a review with special reference to the pharmacopoea Internationalis. Bull. World Health Organ. 4, 577–603.
Väre, T., Nordfors, U., 2025. Early childhood diets in medieval and post-medieval Pälkäne, Finland: insights from stable isotope analysis. J. Archaeol. Sci. Rep. 63, 105113. https://doi.org/10.1016/j.jasrep.2025.105113.
Veselý, L., Ercoli, F., Ruokonen, T.J., Bláha, M., Duras, J., Haubrock, P.J., Kainz, M., Hämäläinen, H., Buřič, M., Kouba, A., 2023. Strong temporal variation of consumer δ13C value in an oligotrophic reservoir is related to water level fluctuation. Sci. Rep. 13, 3642. https://doi.org/10.1038/s41598-023-30849-9.
Von Holstein, I.C.C., Penkman, K.E.H., Peacock, E.E., Collins, M.J., 2014. Wet degradation of keratin proteins: linking amino acid, elemental and isotopic composition: isotopic characterisation of wool hydrolysis. Rapid. Commun. Mass Spectrom. 28, 2121–2133. https://doi.org/10.1002/rcm.6999.
Walter, B.S., DeWitte, S.N., Dupras, T., Beaumont, J., 2020. Assessment of nutritional stress in famine burials using stable isotope analysis. Am. J. Phys. Anthropol. 172, 214–226. https://doi.org/10.1002/ajpa.24054.
Wang, B., Yang, S., Li, P., Qin, C., Wang, C., Ali, M.U., Yin, R., Maurice, L., Point, D., Sonke, J.E., Zhang, L., Feng, X., 2023. Trace mercury migration and human exposure in typical mercury-emission areas by compound-specific stable isotope analysis. Environ. Int. 174, 107891. https://doi.org/10.1016/j.envint.2023.107891.
Wang, T., Fuller, B.T., Jiang, H., Li, W., Wei, D., Hu, Y., 2022. Revealing lost secrets about Yingpan Man and the Silk Road. Sci. Rep. 12, 669. https://doi.org/10.1038/s41598-021-04383-5.
WHO, 1991. Inorganic Mercury (No. 9241571187), Environmental Health Criteria. World Health Organization, Geneva.
WHO, 1990. Methylmercury, Environmental Health Criteria; No. 101. World Health Organization, Geneva.
Wiener, J.G., Suchanek, T.H., 2008. The basis for ecotoxicological concern in aquatic ecosystems contaminated by historical mercury mining. Ecol. Appl. 18. https://doi.org/10.1890/06-1939.1.
Wilson, A.S., Taylor, T., Ceruti, M.C., Chavez, J.A., Reinhard, J., Grimes, V., Meier-Augenstein, W., Cartmell, L., Stern, B., Richards, M.P., Worobey, M., Barnes, I., Gilbert, M.T.P., 2007. Stable isotope and DNA evidence for ritual sequences in Inca child sacrifice. Proc. Natl. Acad. Sci. U.S.A. 104, 16456–16461. https://doi.org/10.1073/pnas.0704276104.
Wu, Y.-S., Osman, A.I., Hosny, M., Elgarahy, A.M., Eltaweil, A.S., Rooney, D.W., Chen, Z., Rahim, N.S., Sekar, M., Gopinath, S.C.B., Mat Rani, N.N.I., Batumalaie, K., Yap, P.-S., 2024. The toxicity of mercury and its chemical compounds: molecular mechanisms and environmental and Human health implications: a comprehensive review. ACS. Omega 9, 5100–5126. https://doi.org/10.1021/acsomega.3c07047.
Yamakawa, A., Nagano, K., Onishi, K., Ukachi, M., Ieda, T., Kobayashi, M., Sano, T., Iwai-Shimada, M., Iwai, K., Inamasu, K., Amouroux, D., Tessier, E., Horvat, M., Alilović, A., Klemenčič, P., Begu, E., Hudobivnik, M.J., Matthew, R., Haraguchi, K., Li, P., Rodríguez-González, P., Suárez-Criado, L., Hu, L., Takeda, N., Li, Y.-F., Uchida, K., 2025. Human hair certified reference material for total mercury, methylmercury, and trace element analyses. Accred. Qual. Assur. 30, 277–290. https://doi.org/10.1007/s00769-025-01637-x.
Zillioux, E.J., 2015. Mercury in fish: history, sources, pathways, effects, and indicator usage. In: Armon, R.H., Hänninen, O. (Eds.), Environmental Indicators. Springer, Netherlands, Dordrecht, pp. 743–766. https://doi.org/10.1007/978-94-017-9499-2_42.
Zvereva, V.V., Trunova, V.A., Sorokoletov, D.S., Polosmak, N.V., 2017. Mercury in archeological hair samples from Xiongnu burials (Noin-Ula, Mongolia): SR XRF and CXRM analysis. X-Ray Spectrom 46, 563–568. https://doi.org/10.1002/xrs.2798.